6.3. Differential diagnostics of biological tissues using method of Stokes-correlometry mapping

A.G. Ushenko, M. Grytsyuk, V.O.Ushenko, G.B. Bodnar,
O. Vanchuliak, A. Antoniv

6.3.1. Theoretical basics and experimental realization of the method of stokes correlometry mapping of biological layers

6.3.1.1. Analytical relations of Stokes correlometry mapping

In the series of research works the possibility of polarimetry diagnostic [1-19] of optically anisotropic layers of biological tissues [20-35] is demonstrated. Along with this, the systemic information about the possibilities of polarimetry in diagnostic of hard system diseases like diabetes is absent.

In this work we make an attempt for obtaining the set of objective criteria of diabetes diagnostics and the estimation of it severity degree. As the ground - we have used a theory of T. Setola, Ya. Tervo and A.T. Friberg [36,37]. It was shown that optical anisotropy of phase-inhomogeneous layer can be described by the phase of the 4th parameter of "two-point" complex Stokes vector.

$$Arg S_4 = arctg\left(\frac{\cos\delta_1 + ctg\rho_2 tg\rho_1 \cos\delta_2}{\sin\delta_1 + ctg\rho_2 tg\rho_1 \sin\delta_2}\right). \qquad (6.3.1)$$

Here ρ - direction of optical axis; δ - phase shift of linear birefringence [38-41].

We have considered a regime of weak phase anisotropy ($\delta_i \le 0{,}12$; $\cos(\delta_1 - \delta_2) \to 1$; $\sin(\delta_1 - \delta_2) \to \delta_1 - \delta_2$). Under these conditions, dependence (6.3.1) takes the form

$$ArgS_4 = arctg\left(\frac{1 + ctg\rho_2 tg\rho_1}{\delta_1 + \delta_2 ctg\rho_2 tg\rho_1}\right). \qquad (6.3.2)$$

It follows from the analysis of the obtained relation (6.3.2) that phase $ArgS_4$ carries information about their birefringence ($\delta(x, y)$).

6.3.1.2. Experimental results of the method of Stokes correlometry

As the test objects we used the histological sections of healthy and affected by diabetes mice internal organs.

The fluorescence of the tissues of mice internal organs was excited by the radiation of semiconductor laser with the wavelength of $\lambda = 0.405\mu m$. The analysis of fluorescent images was performed by means of bandpass filter with the maximum of transmission $\lambda^* = 0.63\mu m$.

Figs. 6.3.1 and 6.3.3 present the coordinate distributions of the value of phase $ArgS_4$, which characterizes the fluorescence of linearly birefringent anisotropic structures of the histological sections of fibrillar kidney tissue (Fig. 6.3.1) and parenchymal tissue of spleen (Fig. 6.3.3).

The set of autocorrelation functions (ACF) [9,17,21-29] of coordinate distributions of the value of phase $ArgS_4$ of the histological sections of healthy and affected by diabetes fibrillar tissue of kidney and parenchymal tissue of kidney was presented in Fig. 6.3.2 and Fig. 6.3.4 correspondingly.

Table 6.3.1 presents the values of correlation moments of the 2nd (half-width of ACF) and the 4th (the kurtosis of ACF) [9,17, 21] of the distributions of phase $ArgS_4$ of the histological sections of this two types.

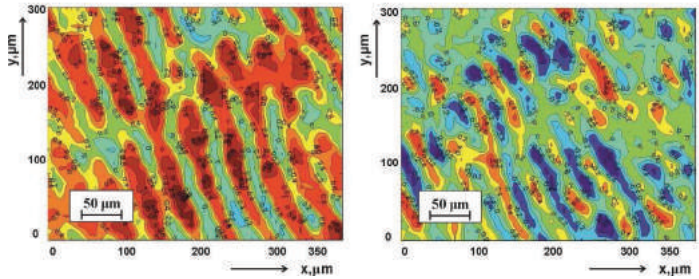

Fig. 6.3.1. Coordinate distributions of the phase values $ArgS_4$ of the 4th parameters of Stokes vector of microscopic images of fluorescence of the histological sections of kidney of healthy mice (fragment (1)) and affected by diabetes (fragment (2)).

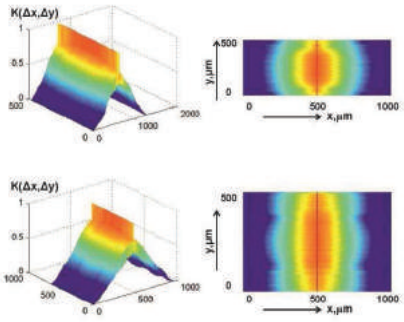

Fig. 6.3.2. Autocorrelation functions of the phase values $ArgS_4$ of the 4th parameters of Stokes vector of microscopic images of fluorescence of the histological sections of kidney of healthy mice (fragment (1, 2)) and affected by diabetes (fragment (3, 4)).

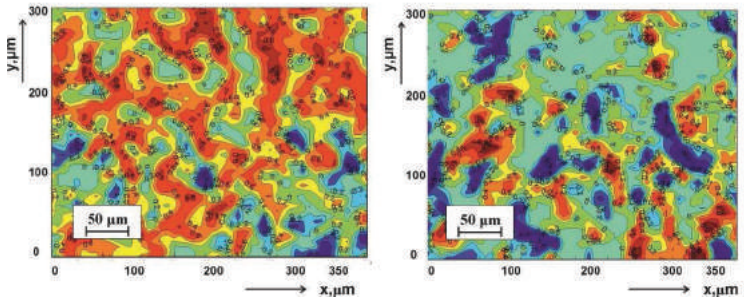

Fig. 6.3.3. Coordinate distributions of the phase values $ArgS_4$ of the 4th parameters of Stokes vector of microscopic images of fluorescence of the histological sections of spleen of healthy mice (fragment (1)) and affected by diabetes (fragment (2)).

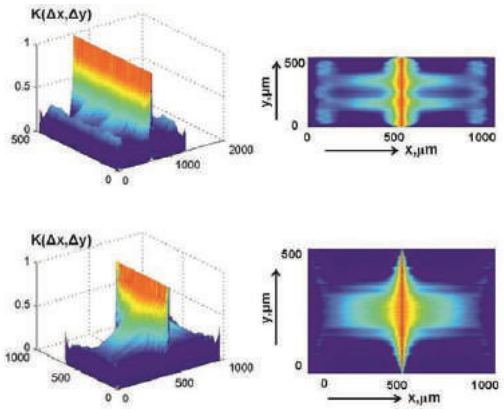

Fig.6.3.4. Autocorrelation functions of the phase values $ArgS_4$ of the 4th parameters of Stokes vector of microscopic images of fluorescence of the histological sections of spleen of healthy mice (fragment (1, 2)) and affected by diabetes (fragment (3, 4)).

Table 6.3.1. Correlation moments of the 2nd (K_2) and the 4th (K_4) orders, which characterize the distributions of the phase $ArgS_4$ of the 4th Stokes vector parameter of microscopic images of fluorescence of the histological sections of healthy and affected by diabetes mice internal organs

Tissue	Fibrillar tissue of kidney		Parenchymal tissue of spleen	
Condition	Normal	Diabetes	Normal	Diabetes
K_2	0.13	0.21	0.19	0.25
K_4	1.31	0.83	0.91	0.56

It was defined an individual sensitivity of correlation moments of the 2nd (K_2) and the 4th (K_4) orders, which characterize the distributions of values of the phase of the 4th Stokes vector parameter $ArgS_4$ of microscopic images of fluorescence of the histological sections of healthy and affected by diabetes mice internal organs.

It was found that more pronounced differences between physiologically states of mice internal organs exist for K_4 - kidney in 1.55times; spleen in 1.48 times.

6.3.2. Clinical application of stokes correlometry in differential diagnostics of diabetes severity degree

6.3.2.1. Object of investigations

Two groups of samples of histological sections of mice spleen tissue were used:

- diabetes (11 days) – group 1 (33 samples);
- diabetes (21 days) - group 2 (33 samples).

Histological sections were produced due to the standard technique on the freezing microtome.

6.3.2.2. Experimental results

Fig. 6.3.5 illustrates the results of Stokes correlometry mapping of the phase of the 4th parameter of Stokes vector $ArgS_4$ of microscopic images of fluorescence of the histological sections of spleen tissue with different time of diabetes existence.

Fig. 6.3.6 presents the autocorrelation functions of coordinate distributions of the value of phase of the 4th parameter of Stokes vector $ArgS_4$ of microscopic images of fluorescence of the histological sections of spleen.

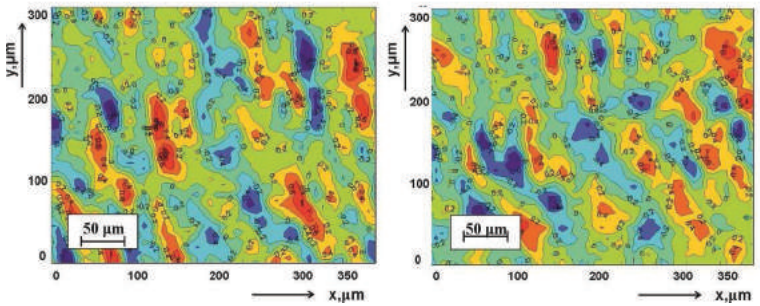

Fig. 6.3.5. Coordinate distributions of the phase values $ArgS_4$ of the 4th parameters of Stokes vector of microscopic images of fluorescence of the histological sections of spleen of mice affected by diabetes (12 days - fragment (1)) and (21 days - fragment (2)).

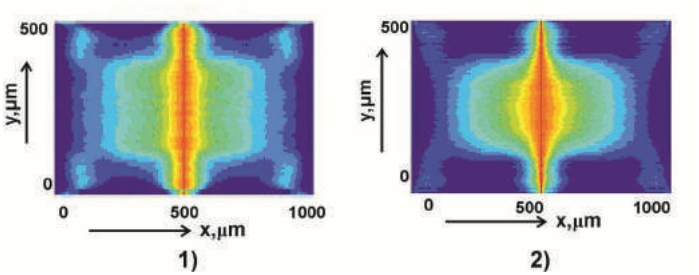

Fig. 6.3.6. Autocorrelation functions of the phase values $ArgS_4$ of the 4th parameters of Stokes vector of microscopic images of fluorescence of the histological sections of spleen of mice affected by diabetes (12 days -fragment (1) and (21 days - fragment (2).

Table 6.3.2 consists of the values of correlation moments of the 2nd (ACF half-width) and the 5th (ACF kurtosis) of the distribution of phase values $ArgS_4$ of microscopic images of spleen tissue samples of both groups.

Table 6.3.2. Correlation moments of the 2nd (K_2) and the 4th (K_4) orders, which characterize the distributions of the phase $ArgS_4$ of the 4th Stokes vector parameter of microscopic images of fluorescence of the histological sections of spleen tissue with diabetes

Tissue	Parenchymal spleen tissue	
Condition	Diabetes (11 days)	Diabetes (21 days)
K_2	0.17 ± 0.08	0.23 ± 0.013
K_4	1.09 ± 0.061	0.67 ± 0.036

For the possible clinical application of the Mueller matrix mapping method for each group of samples the operating characteristics, typical for

evidence-based medicine [42-44] that determine the diagnostic power of the method are determined, namely – sensitivity ($Se = \frac{a}{a+b}100\%$), specificity ($Sp = \frac{c}{c+d}100\%$) and balanced accuracy ($Ac = \frac{Se+Sp}{2}$), where a and b – the number of correct and incorrect diagnoses within group 2; c and d – the same within group 1 – Table 6.3.2.

For the correlation moment of the 4th order it was reached the level of balanced accuracy ($Ac = 95\%$).

6.3.3. Conclusions

Short theoretical basics of the method of differential Stokes correlometry mapping of microscopic images of fluorescence of polycrystalline structure of the histological sections of mice spleen tissue were provided. It was demonstrated the results of experimental approbation of such method. The differentiation of linear birefringence of spleen tissue with different diabetes severity degree was realized. It was reached an excellent levels of balanced accuracy of differential diagnostics of such a samples.

References

1. G. Müller et al., Eds., *Medical Optical Tomography: Functional Imaging and Monitoring*, Vol. IS11, SPIE Press, Bellingham, Washington (1993).

2. Yao G. Two-dimensional depth-resolved Mueller matrix characterization of biological tissue by optical coherence tomography / G. Yao, L. V. Wang // Opt. Lett. – 1999. – V. 24. – P. 537-539.

3. Lu S. Interpretation of Mueller matrices based on polar decomposition / S. Lu, R. A. Chipman // J. Opt. Soc. Am. A. –1996. – Vol. 13. – P.1106-1113.

4. V. V. Tuchin, “Light scattering study of tissues,” Physics-Uspekhi 40(5),

495–515 (1997).

5. Angelsky, O. V., Bekshaev, A. Ya., Maksimyak, P. P., Maksimyak, A. P., Hanson, S. G., Zenkova, C. Yu., "Self-diffraction of continuous laser radiation in a disperse medium with absorbing particles," Optics Express 21(7) 8922-8938, (2013).

6. Angelsky, O. V., Bekshaev, A. Ya., Maksimyak, P. P., Maksimyak, A. P., Hanson, S. G., Zenkova, C. Yu., "Self-action of continuous laser radiation and Pearcey diffraction in a water suspension with light-absorbing particles," Optics Express 22(3) 2267-2277, (2014).

7. Angelsky, O. V., Bekshaev, A. Ya., Maksimyak, P. P., Maksimyak, A. P., Hanson, S. G.,"Measurement of small light absorption in microparticles by means of optically induced rotation," Optics Express 23(6) 7152-7163, (2015).

8. Polyanskii, V.K., Angelsky, O.V., Polyanskii, P.V., "Scattering-induced spectral changes as a singular optical effect," Optica Applicata 32 (4), 843-848 (2002).

9. Angelsky, O.V., Besaha, R.N., Mokhun, A.I., Mokhun, I.I., Sopin, M.O., Soskin, M.S., "Singularities in vectoral fields," Proc. SPIE, 40-54, (1999) .

10. OV Angelsky, YY Tomka, AG Ushenko, YG Ushenko, SB Yermolenko, "2-D tomography of biotissue images in pre-clinic diagnostics of their pre-cancer states," Proc. SPIE. 5972, 158-162 (2005).

11. Angel'skiĭ, O.V., Ushenko, A.G., Ermolenko, S.B., Ushenko, Yu.A., Pishak, O.V., "Polarization Based Visualization of Multifractal Structures for the Diagnostics of Pathological Changes in Biological Tissues," 2000 Optics and Spectroscopy (English translation of Optika i Spektroskopiya) 89 (5), 799-804 (2000).

12. Ushenko, A.G. "Polarization Correlometry of Angular Structure in the Microrelief Pattern of Rough Surfaces," Optics and Spectroscopy (English translation of Optika i Spektroskopiya) Opt. Spectrosc. 92, 227–229 (2002) .

13. Ushenko, A.G., Burkovets, D.N., Ushenko, Yu.A. “Polarization Phase Mapping and Reconstruction of Biological Tissue Architectonics during Diagnosis of Pathological Lesions,” Optics and Spectroscopy (English translation of Optika i Spektroskopiya), 93 (3), 449-456, (2002).

14. Angelsky, O.V., Ushenko, A.G., Ushenko, Y.G. “Complex degree of mutual polarization of biological tissue coherent images for the diagnostics of their physiological state,”Journal of Biomedical Optics, 10 (6), 060502-060502-3, (2005).

15. Holovatsky, V.A., Makhanets, O.M., Voitsekhivska, O.M. “Oscillator strengths of electron quantum transitions in spherical Nanosystems with donor impurity in the center,” Physica E: LowDimensional Systems and Nanostructures 41(8), 1522–1526 (2009).

16. S. L. Jacques, “Polarized light imaging of biological tissues” in Handbook of Biomedical Optics, D. Boas, C. Pitris, and N. Ramanujam, Eds., pp. 649–669, CRC Press, Boca Raton, London, New York (2011).

17. Y.A. Ushenko, T.M. Boychuk, V.T. Bachynsky, O.P. Mincer, “Diagnostics of Structure and Physiological State of Birefringent Biological Tissues: Statistical, Correlation and Topological Approaches” in Handbook of Coherent-Domain Optical Methods, ISBN 978-1-4614-5175-4. Springer Science+Business Media New York, 2013, p. 107-148.

18. T. Vo-Dinh, Ed., Biomedical Photonics Handbook, 2nd ed., CRC Press, Boca Raton (2014).

19. V. V. Tuchin, Tissue Optics: Light Scattering Methods and Instruments for Medical Diagnostics, 3rd ed., Vol. PM 254, SPIE Press, Bellingham, Washington (2015).

20. Brus, V.V., Pidkamin, L.I.,Arkhelyuk, A.D., “The effect of CoO impurity and substrate temperature on optical properties of TiO 2 thin films,” Proc. SPIE 8338, 83381A (2011).

21. Dubolazov, A. V., Marchuk, V., Olar, O. I., Bachinskiy, V. T., Vanchuliak, O. Y., Pashkovska, N. V., Kostiuk, S. V., “Multiparameter correlation microscopy of biological fluids polycrystalline networks,” In Eleventh International Conference on Correlation Optics, International Society for Optics and Photonics, pp. 90661Y-90661Y (2013).

22. Ushenko, O., Dubolazov, A., Balanets' ka, V., Karachevtsev, A., Sydor, M., "Wavelet analysis for polarization inhomogeneous laser images of blood plasma," Proc. SPIE. Vol. 8338 (2011).

23. Yu. A. Ushenko, V. A. Ushenko, A. V. Dubolazov, V. O. Balanetskaya, N. I. Zabolotna, “Mueller-matrix diagnostics of optical properties of polycrystalline networks of human blood plasma,” Optics and Spectroscopy 112(6), 884-892 (2012).

24. Yu. A. Ushenko, A. V. Dubolazov, V. O. Balanetskaya, A. O. Karachevtsev, V. A. Ushenko, “Wavelet-analysis of polarization maps of human blood plasma,” Optics and Spectroscopy 113(3), 332-343 (2012).

25. Angelsky, P. O., Ushenko, A. G., Dubolazov, A. V., Sidor, M. I., Bodnar, G. B., Koval, G., Trifonyuk, L., “The singular approach for processing polarization-inhomogeneous laser images of blood plasma layers,” Journal of Optics, 15(4), 044030 (2013).

26. Dobrovolsciy, Yu. G., G Perevertaylo, V. L., Shabashcevich, B. G., Pidkamin, L. J., “Clarifying coverages on the basis of tapes SnO2, SiO2, Si3N4 for photodiodes of ultraviolet and visible range,” Proc. SPIE 7388, (2009).

27. A.G. Ushenko, N.V. Pashkovskaya, O.V. Dubolazov, Yu.A. Ushenko, Yu.F. Marchuk, V.A. Ushenko, “Mueller matrix images of polycrystalline films of human biological fluids,” Romanian reports in physics 67(4), 1467-1479 (2015).

28. V. P. Prysyazhnyuk, Yu. A. Ushenko, A. V. Dubolazov, A. G. Ushenko, and

V. A. Ushenko, “Polarization-dependent laser autofluorescence of the polycrystalline networks of blood plasma films in the task of liver pathology differentiation,” Appl. Opt. 55, B126-B132 (2016).

29. A. V. Dubolazov, N. V. Pashkovskaya, Yu. A. Ushenko, Yu. F. Marchuk, V. A. Ushenko, and O. Yu. Novakovskaya, “Birefringence images of polycrystalline films of human urine in early diagnostics of kidney pathology,” Appl. Opt. 55, B85-B90 (2016).

30. Ushenko, A.G. “Laser diagnostics of biofractals,” Quantum Electronics, 29 (12), 1074-1077 (1999).

31. Angelsky, O.V., Polyanskii, P.V., Hanson, S.G., “Singular optical coloring of regularly scattered white light,” Optics Express 14 (17), 7579-7586 (2006).

32. Angel'skiĭ, O.V., Ushenko, A.G., Arkhelyuk, A.D., Ermolenko, S.B., Burkovets, D.N., “Structure of matrices for the transformation of laser radiation by Biofractals,” Quantum Electronics 29 (12), 1074-1077 (1999).

33. Angelsky, O.V., Hanson, S.G., Maksimyak, P.P., Maksimyak, A.P., Zenkova, C.Yu., Polyanskii, P.V., Ivanskyi, D.I., “Influence of evanescent wave on birefringent microplates,” Optics Express 25(3) 2299-2311 (2017).

34. Angelsky, O.V., Gorky, M.P., Hanson, S.G., Lukin, V.P., Mokhun, I. I., Polyanskii, P.V., Ryabiy, P.A., “Optical correlation algorithm for reconstructing phase skeleton of complex optical fields for solving the phase problem,” Opt. Exp. 22(5), 6186-6193 (2014).

35. Angelsky, O.V., Maksimyak, A.P., Maksimyak, P.P., Hanson, S G., "Interference diagnostics of white-light vortices," Opt. Express 13, 8179-8183 (2005).

36. J. Tervo, T. Setala, A. Friberg, “Degree of coherence for electromagnetic fields,” Opt. Express 11, 1137-1143 (2003).

37. J. Tervo, T. Setala, A. Friberg, “Two-point Stokes parameters: interpretation and properties," Optics Letters 34(20), 3074-3076 (2009).

38. Ushenko, Yu. A., M. P. Gorskii, A. V. Dubolazov, A. V. Motrich, V. A. Ushenko, M. I. Sidor “Spatial-frequency Fourier polarimetry of the complex degree of mutual anisotropy of linear and circular birefringence in the diagnostics of oncological changes in morphological structure of biological tissues,” Quantum Electron 42(8), 2012.

39. Brus, V.V., Pidkamin, L. J., Ilashchuk, M.I., Maryanchuk, P.D., “Propolis films for hybrid biomaterial-inorganic electronics and optoelectronics,” Appl. Opt. 53, B121-B127 (2014).

40. Mikhailova, A.D., Yermolenko, S.B., Zimnyakov, D.A., Angelsky, O.V., “Aging-Caused Changes in Optical Anisotropy of Fibrous Tissues,” Proc. SPIE, 7388, 738819-1–738819-8 (2009).

41. Yu. A. Ushenko, V. T. Bachynsky, O. Ya. Vanchulyak, A. V. Dubolazov, M. S. Garazdyuk, and V. A. Ushenko, “Jones-matrix mapping of complex degree of mutual anisotropy of birefringent protein networks during the differentiation of myocardium necrotic changes,” Appl. Opt. 55, B113-B119 (2016).

42. Cassidy, "Basic concepts of statistical analysis for surgical research," Journal of Surgical Research 128, 199-206 (2005).

43. C. S. Davis, Statistical methods of the analysis of repeated measurements, 744, New York: Springer-Verlag (2002).

44. A. Petrie, B. Sabin, Medical Statistics at a Glance, pp. 157, Blackwell Publishing (2005).